Current Continuity in Auroral System Science:

A 3-D Modelling Approach to Current Closure in Non-Sheetlike Auroral Arcs

A Thesis Proposal

Submitted to the Faculty

in partial fulfillment of the requirements for the

degree of

Doctor of Philosophy

in

Physics

by

Jules van Irsel

DARTMOUTH COLLEGE

Hanover, New Hampshire

May 4, 2022

Examining Committee:

(Chair) Kristina A. Lynch

Yi-Hsin Liu

James W. LaBelle

Abstract

The local coupling of the Earth's ionosphere and the magnetosphere (MI) is an open area of study. A common context is to view the magnetosphere to have certain demands of field aligned currents (FAC) or perpendicular flow patterns to which the ionosphere responds. In the electrostatic case, this response can be simplified to satisfying current closure, the path of which is dictated by the ionospheric conductivity (Paschmann et al., 2003; Wolf, 1975; Brekke, 1989; Kelley, 2009).

$$j_{\parallel}(x,y) = \Sigma_P \nabla_\perp \cdot \mathbf{E}_\perp + \mathbf{E}_\perp \cdot \nabla_\perp \Sigma_P - (\mathbf{E}_\perp \times \hat{\mathbf{s}}) \cdot \nabla_\perp \Sigma_H,$$

where $j_\parallel$ is a 2-D horizontal map of FAC at the topside ionosphere, $\mathbf{E}_\perp$ is the ionospheric electric field with $\mathbf{v}_\perp = \mathbf{E}_\perp \times \mathbf{B}_0/B_0^2$, and Σ_P and Σ_H are the height integrated Pedersen and Hall conductivities. This tells us that, given a 2-D horizontal map of FAC (or perpendicular flow) and with knowledge of the ionosphere's conductances, one can find a solution for the electric field (or FAC). The conductivity, however, depends strongly on the precipitation spectrum via impact ionization (Evans, 1974; Fang et al., 2010; Grubbs et al., 2018; Solomon, 2017). Additionally, straggling recombination and perpendicular transport can induce a hysteresis of precipitation dynamics. Because of these factors, it is not well understood how the ionospheric system "chooses" its response and, especially for non-idealized arc structures, finding the physical solution is non-trivial.

The aim of this thesis is to find physical, self-consistent solutions to the ionospheric current continuity equation using state-of-the-art ionospheric 3-D modelling to provide insight into the role the ionosphere plays in MI coupling for less idealized auroral events. In particular, knowing the portions of FAC closed by Pedersen currents, which produce collisional Joule heating, versus Hall currents, which are non-dissipative (Amm et al., 2008; Clayton et al., 2021), gives insight into the extent to which the ionosphere acts as a load to a magnetospheric generator (Wygant et al., 2000).

For idealized sheet-like auroral arcs, those with minimal longitudinal variation, this is a relatively well-posed and constrained problem (Richmond, 2010). The interest of this thesis lies in determining the limitations of this idealized morphology by introducing along-arc structure and using 3-D simulations of the auroral ionosphere produced by the Geospace Environment Model of Ion-Neutral Interactions (GEMINI) (Zettergren and Semeter, 2012; Zettergren et al., 2015). Placing the model input boundary conditions at the topside ionosphere, a 2-D map of either FAC or electric potential

along with a 2-D map of electron precipitation drives the model space. A rich set of illustrative cases based on statistics (Mule, A., Kawamura, M. S.) of both satellite (FAST, SWARM, etc.) and ground-based (THEMIS-GBO, REGO, etc.) data will be used to develop these maps. A substantial part of this project will include creating tools to properly visualize the inherent 3-dimensionality of the ionospheric current system. The *317 Lynch Rocket Lab* team will aid in this development.

Overall, this description of electrostatic MI coupling is only valid up to time scales of ∼100 s (Lotko, 2004; Richmond, 2010). Lotko (2004) describes a model that allows for limited dynamics (time scales of 10 s) by including inductive MI coupling while retaining quasistatics. An additional component of this thesis will be to modularly add this physics to GEMINI in order to implement relevant Alfvénic effects. A second module to be possibly added to GEMINI would include a bookkeeping of energy flow for the implementation of Poynting theorem constraints (Richmond, 2010).

This work will strive toward better use of the abundance of all-sky imagery data available, supplemented by in-situ data and modelling, by means of systematically exploring the third dimension in auroral system science; the ultimate aim is to be able to "read the aurora" by simply looking at their visible signatures.

Contents

1 Background and Motivation

1.1 "Local" Magnetosphere-Ionosphere Coupling

The aurora are likely the earliest evidence of a connection to the Sun and our atmosphere, mediated through the Earth's magnetic field (see Anders Celsius and Olav Hiorter's work from 1747 (Paschmann et al., 2003)). Yet, they are displayed at the terminal end of a very complex system governed by highly non-linear plasma physics, which is referred to as auroral system science. But, beautiful as they are, the aurora themselves are only the visible portion of this system. The morphology, color, and dynamics of the aurora are all the result of an interplay of electromagnetic fields, currents, collisional interactions, etc., all within the partly ionized layer of our atmosphere, i.e. the ionosphere.

This connection, or coupling, ultimately is driven by the Sun, but let's consider the region where the Solar wind touches the outer magnetosphere as an intermediary. This context is what's often referred to as magnetosphere-ionosphere (MI) coupling (Wolf, 1975; Cowley, 2000; Lotko, 2004). The global, quasi-static picture for electric field coupling is the two cell convection pattern, first outlined by Dungey (1961) and further explained by Paschmann et al. (2003), Section 8.3. This $\mathbf{E} \times \mathbf{B}$ drift cycle of dayside geomagnetic field lines disconnecting to the IMF, draping anti-Sunward, reconnecting to the IMF, and dipolarizing while drifting back to the dayside, has electric fields that map down to the polar cap via the equipotential field lines. But, the ionosphere is not a passive component in this mapping.

In addition to convection, there is a coupling through field-aligned currents (FAC), a.k.a. Birkeland currents, which come in up-down pairs. Out in the magnetosphere, any deviation from a dipolar magnetic field will require currents to sustain, simply by Ampere's law. These FAC pairs arise because such magnetospheric currents need to close and the collisional ionosphere is the easiest path to do so. However, the path of closure depends strongly on the ionospheric response to, not just the electric fields, but also auroral precipitation and E/F region ionospheric transport processes. This precipitation is longitudinally aligned, dynamic, and highly structured, such that this closure path is non-trivial.

Given the dictation of electric fields and FACs by the magnetospheric driver, it's not uncommon to adapt an electric circuit description. With this, the driver is considered an electric generator with

$\mathbf{j} \cdot \mathbf{E} < 0$ which is balanced by dissipation in either the acceleration region, or inside the ionosphere itself via Pedersen currents, but more on this later. Lysak (1985) considers such a description and investigates the overall effects between the two limiting cases where a generator holds a steady current, or one that holds a steady voltage. While the generator mechanism itself is outside of our scope, he concludes that the resulting auroral currents change their natural scale lengths depending on whether the voltage or current drivers dominate. Furthermore, in-situ spacecraft measurements have shown directly that both flow and FAC can be highly structured, embedded within the larger scale current system (Archer et al., 2017; Lühr et al., 2015; Rother et al., 2007; Sugiura et al., 1982). The auroral system science governing these mesoscale (1s - 100s of km) structures is what is meant by local MI coupling. In terms of time scales, this work will primarily focus on DC coupling with some steps toward Alfvénic behavior.

1.2 Discrete Auroral Precipitation

Apart from electric field and current coupling, a third mechanism relevant to this context is the "acceleration region", placed at 1-2 R_E above the ionosphere and below the magnetospheric driver. Quiet, discrete auroral arcs (Karlsson et al., 2020) are the result of precipitating electrons which have been accelerated through a U-shaped potential (the U-shape resulting from having a parallel potential drop on field lines that prefer to be equipotential). It's theorized that this potential forms in low density regions (night-side) in order to accelerate charge carriers into the loss cone to accommodate current demands at these altitudes on these field lines (Knight, 1973; Temerin and Carlson, 1998).

A method of sustaining such a parallel electric field is through *double layers* at the bottom end of the acceleration region. Double layers are *Debye sheaths* which consist of two parallel layers of opposite charge sustained, ultimately, by the order of magnitude difference in electron and ion temperatures (Ergun et al., 1998; Paschmann et al., 2003).

A 3-D model of the acceleration region including electron dispersion by Seyler (1990) shows that steady-state superposed oblique Alfvén waves can also develop a parallel electric field, along with thin, structured current sheets. This again adds to the local MI coupling scene with respect to the scale sizes involved in this precipitation mechanism. This work does not, however, focus on the mechanism of sustaining the parallel electric field. Ultimately, this parallel potential drop creates a

known electron differential number flux pattern, including thermal, beaming, and secondary components (Fang et al., 2010; Evans, 1974). This electron spectrum is known as inverted-V precipitation based on the pointed shape of the electron energy in spectrograms. Alfvénic acceleration adds a broadband part with narrow pitch angle to this spectrum (Paschmann et al., 2003). This energy provides density enhancements in the lower ionosphere via impact ionization which directly affect the ionosphere's ability to carry current, i.e. the ionospheric conductivity.

These U-shaped potentials are generally longitudinally aligned ridges on the two-cell polar cap potential. The precipitation they produce has strong gradients, it can appear and stretch out west or eastward, it can strengthen and reach deeper into the ionosphere, it can wiggle and bend. The ionospheric conductivity is very sensitive to this precipitation, so this local morphology directly controls the current continuity.

1.3 Ionospheric Ohm's Law and Current Continuity

Up until this point we've isolated the local MI coupling problem to quasi-electrostatic, mesoscale electric fields, FAC, and ionospheric conductivity. To determine the manner in which the ionosphere can respond to these variables, the ionospheric Ohm's law is applied along with current continuity. Following the derivation in chapter 8 by Kelley (2009), we start with steady-state current closure and split it into its parallel and perpendicular parts,

$$\nabla \cdot \mathbf{j} = \nabla_\perp \cdot \mathbf{j}_\perp + \frac{\partial j_\parallel}{\partial s} = 0, \tag{1}$$

where $\mathbf{j}$ is the full current density and s is the parallel coordinate. If we integrate this over the heights where perpendicular currents exist, we obtain the expression

$$j_\parallel = \int_{s_1}^{s_0} \mathrm{d}s \nabla_\perp \cdot \mathbf{j}_\perp \tag{2}$$

with $s_0 \approx 80$ km and $s_1 \approx 200$ km. Next, using Ohm's law, we write

$$\mathbf{j} = \sigma \cdot (\mathbf{E} + \mathbf{U} \times \mathbf{B}), \tag{3}$$

with σ the conductivity tensor, $\mathbf{U}$ the neutral wind velocity, and $\mathbf{B}$ the magnetic field. In our context, the effects and general dynamics of the neutral winds can be a minor offset of ∼10% (Fraunberger et al., 2020), so we let $\mathbf{U} = 0$. This gives $\mathbf{j}_\perp = \sigma_\perp \cdot \mathbf{E}_\perp$ and thus

$$j_\parallel = \int_{s_1}^{s_0} \mathrm{d}s \nabla_\perp \cdot (\sigma_\perp \cdot \mathbf{E}_\perp). \tag{4}$$

Since the divergence is orthogonal to s, and the electric field is constant (equipotential field lines) along the path of integration we may write

$$j_\parallel = \nabla_\perp \cdot (\mathbf{\Sigma}_\perp \cdot \mathbf{E}_\perp), \quad \text{with} \quad \mathbf{\Sigma}_\perp = \begin{pmatrix} \Sigma_P & -\Sigma_H \\ \Sigma_H & \Sigma_P \end{pmatrix}, \tag{5}$$

where Σ_P and Σ_H are the height integrated Pedersen and Hall conductivities, a.k.a. conductances. Rearranging this gives

$$j_\parallel = \Sigma_P \nabla_\perp \cdot \mathbf{E}_\perp - \Sigma_H \nabla_\perp \cdot (\mathbf{E}_\perp \times \hat{\mathbf{s}}) + \mathbf{E}_\perp \cdot \nabla_\perp \Sigma_P - (\mathbf{E}_\perp \times \hat{\mathbf{s}}) \cdot \nabla_\perp \Sigma_H. \tag{6}$$

If for the moment we work in Cartesian coordinates we find that the second term on the right hand side has the product $\partial_x E_y - \partial_y E_x = (\nabla \times \mathbf{E})_z \equiv \partial_t B_\parallel$, which for quasi-electrostatics is negligible. This then yields a 2-D map of field aligned current in the ionosphere (ending the derivation by Kelley (2009)):

$$j_\parallel = \Sigma_P \nabla_\perp \cdot \mathbf{E}_\perp + \mathbf{E}_\perp \cdot \nabla_\perp \Sigma_P - (\mathbf{E}_\perp \times \hat{\mathbf{s}}) \cdot \nabla_\perp \Sigma_H. \tag{7}$$

This expression tells us that there are three sources and sinks for ionospheric FAC. 1) Diverging electric fields, which can be thought of as electric field shocks for elongated structures. By Gauss' law, this term accounts for the removal of charge build-up or depletion in order to keep $\partial_t \rho = 0$. 2) Gradients in Pedersen conductances in the direction of the ionospheric electric field. Again, for the elongated U-shaped potentials, this often means gradients in the across-arc direction. 3) Gradients in Hall conductance in the direction perpendicular to the electric field. This term is often ignored, especially in the 2-D picture, as gradients in this direction are negligible for sheet-like arcs.

What's meant by sheet-like arcs is thin (1s - 10s of km), long (100s of km), auroral sheets of roughly constant latitude. For quiet, discrete, growth-phase arcs this is a great description and the

system is relatively well-posed, but this only accounts for a subset of auroral arcs. Our interest lies in the likely event that along-arc structure is introduced to this picture, at which point the self-consistent, physical solution to Eq. (7) is a much less trivial problem and more one that involves a complete picture of the 3-D system.

1.4 3-D Modelling: Why now?

Given the relative simplicity of sheet-like arcs and their abundance in auroral system science, early models naturally focused on 1- and 2-D systems (Goertz and Boswell, 1979; Mallinckrodt, 1985). In addition, early measurements were either 1-D (e.g. field-aligned incoherent scatter radars) or 2-D, such as networks of magnetometers measuring perpendicular currents like the electrojet. However, with recent missions including ground-based observatories such as THEMIS-GBO, REGO, etc., in conjunction with spacecrafts like CHAMP, SWARM, etc., the 3-D picture has become much more accessible.

Amm et al. (2008) outline several outstanding questions that can be addressed by the modelling of high-latitude ionospheric electrodynamics in 3-D. They focus on ionospheric induction for MI coupling, ionospheric current closure and the *Cowling channel*, and mesoscale thermospheric coupling. This work will largely focus on ionospheric current closure, but also inductive MI coupling further down the line. The basic Cowling channel involves an east-west aligned band of enhanced conductivity in the ionosphere which, with an imposed background electric field, creates both Pedersen and Hall currents which can polarize at the edges of the channel creating secondary electric fields with associated currents (Paschmann et al., 2003). Amm et al. (2008) investigate a limited 3-D version of this channel where the layers of Pedersen and Hall currents are at their respective conductivity peak altitudes, with FAC closure at the northern and southern boundaries of the channel. Figure 1 by Fujii et al. (2011) illustrates this system, but they've taken it a step further where the current layers are closed also at the eastern and western boundaries. This gives diverging, i.e. overflowing, Hall and Pedersen currents the option to close in much more complex ways, such as the development of vertical current loops. 2-D simulations allowing for altitude dependent conductivities have shown such loops (Mallinckrodt, 1985), however, a true description of the 3-D path that current follows is still an open area of study.

A better understanding of closure through Pedersen versus Hall current enables understanding

of the role played by the ionosphere as a load in the circuit description. The primary means of dissipating energy in the ionosphere are through Joule heating, i.e. Pedersen current with $\mathbf{j}_P \cdot \mathbf{E}_\perp > 0$, or via ion-neutral frictional drag, i.e. the neutral wind dynamo (which we're ignoring in this work), but not through Hall current as $\mathbf{j}_H \cdot \mathbf{E}_\perp = 0$ (Kaeppler et al., 2012; Fujii et al., 2011; Wygant et al., 2000; Clayton et al., 2021). Furthermore, the parallel electric field contributes to energy exchange, $E_\parallel j_\parallel$, emphasising the coupling introduced by accelerated precipitation.

Recent, more advanced 2-D modelling of the ionosphere, including ion heating, perpendicular transport, molecular ion generation, etc., by Zettergren and Semeter (2012) shows the timescale discrepancy between plasma transport and recombination can cause a hysteresis of electron precipitation via impact ionization. This explains that DC dynamics of precipitation can develop more involved conductivity gradients in the along-arc direction as well. Zettergren et al. (2015) extended this model to include the third dimension in an effort to study the dynamics of density cavities generated by frictional heating.

Marghitu (2012) reviews auroral arc electrodynamics as they were understood around a decade ago. They focus on 1-D thin (in altitude) and uniform (in longitude) arcs, 2-D thin and non-uniform arcs, as well as 2-D thick uniform arcs as described by Fujii et al. (2011). With the aid of 1-D spacecraft in-situ data, they develop a tentative model a of 3-D arc during the Dungey cycle (Dungey, 1961) using these three descriptions but ultimately allude to the fact that "arc models in one or two dimensions are able to capture some of the observed ionospheric features, but a complete 3D description is still to be developed" (Marghitu, 2012).

2 Thesis Statement

The scope of this work will address the incomplete description of auroral arcs that stray from their basic, sheet-like morphology. The aim is to find physical, self-consistent solutions to the ionospheric current continuity equation, Eq. (7), using state-of-the-art ionospheric 3-D modelling to provide insight into the role the ionosphere plays in MI coupling for less idealized auroral events. In particular, knowing the portions of FAC closed by Pedersen currents, which produce collisional Joule heating, versus Hall currents, which are non-dissipative, gives insight into the extent to which the ionosphere acts as a load to a magnetospheric generator. Secondary to this, the extent to which

inductive MI coupling effects this electrostatic picture will be investigated.

Section 3 outlines the tools, approach, and methodology that will be used to address this thesis statement including a description of the model used, how it will be driven, and the tools used to interpret the output. Section 4 describes a preliminary set of science studies that will be done using these tools and methods, as well as the specific science questions they will address and a path to science closure. Section 5 provides a basic timeline of concrete tasks and goals this thesis will aim to achieve.

3 Approach and Methodology

3.1 The 3-D GEMINI Model

This work will make use of the Geospace Environment Model of Ion-Neutral Interactions (GEMINI). This model has evolved from its first published use in Zettergren and Semeter (2012) as a 2-D MATLAB code after which it has undergone substantial improvements. More recently, for use by Zettergren et al. (2015), it was translated to FORTRAN along with message passing interface (MPI) parallelization to allow for fully 3-D simulations. This is a multi-fluid model (6 ion + electron), that's quasi-electrostatic with its particle continuity including chemical production/loss and photo/impact ionization. Parallel ion momentum density has a full time-dependent treatment including gravity and ion-ion/ion-neutral collisions, but excluding ion stress. Perpendicular ion momentum density is treated as a steady state solution. Ion energy density is fully time-dependent including thermal conduction heat flux and collisional heating. For electrons, the mass and momentum densities are solved through quasi-neutrality and the definition of current density. The electron energy density is treated much like the ions, but also including thermoelectric heat flux and inelastic cooling/heating from photoelectrons.

This fluid description is supplemented with Maxwell's equations and, at the time of writing, includes no displacement current or magnetic induction effects. With this and the above fluid description, the solution used to determining the electric field (or parallel current) is through having divergence-less currents (or curl-free electric fields) and invoking Ohm's law.

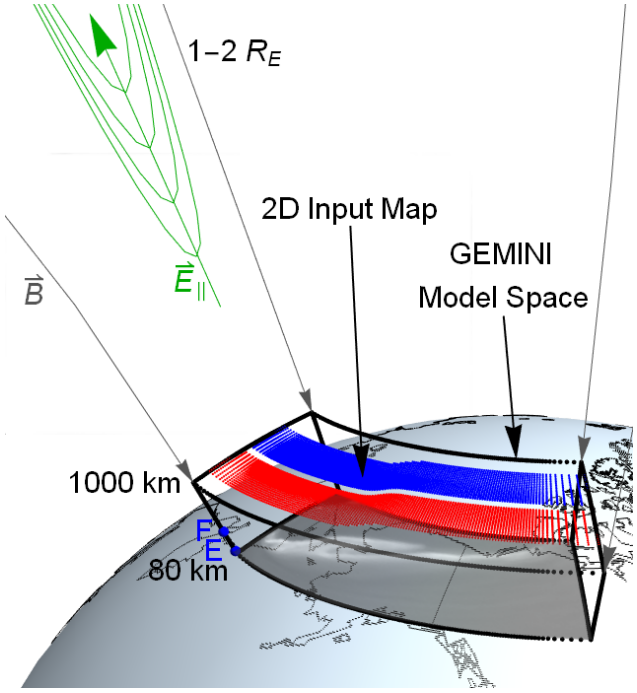

Figure 1: The general framework and context of this work, and its use of the GEMINI model. The dotted black box depicts the GEMINI model space over Alaska from 80 km to ∼1000 km in altitude. The approximate E and F region peaks are shown on the side in blue. The U-shaped potential/parallel electric field is shown in green at around 1-2 R_E (almost to scale). The magnetic field lines connecting to the magnetospheric generator region are shown in gray. The top of the model space shows an example of a 2-D input map of FAC and the bottom shows roughly where auroral emission lies.

3.2 Data Based 2-D Driving Maps

Figure 1 illustrates the context in which this work will use GEMINI. The model space spans around 3000 km east-west, 1000 km north-south, and around 1000 km in altitude, from the lower E region to the topside F region. The magnetic field inside the model space is aligned with the radial coordinate, $\hat{\mathbf{e}}_1$, and is constant. The model is driven with 2-D, time-dependent maps of total precipitation energy flux, Q, and characteristic energy, E_0, to cover the impact ionization via calculations described in Fang et al. (2010). This driver exists at the topside of the model space, which is located below the auroral acceleration region at around 1000 km. In addition to this, the model can be driven with a map of FAC (as shown in Figure 1) or perpendicular plasma flow in the form of a potential map.

Figure 2 and 3 collectively show an example of such an input. This particular one has a slight along-arc bend in its profile with a constant band of low intensity precipitation embedded in an upward current sheet that's poleward of an accompanying return current sheet. If instead, this run

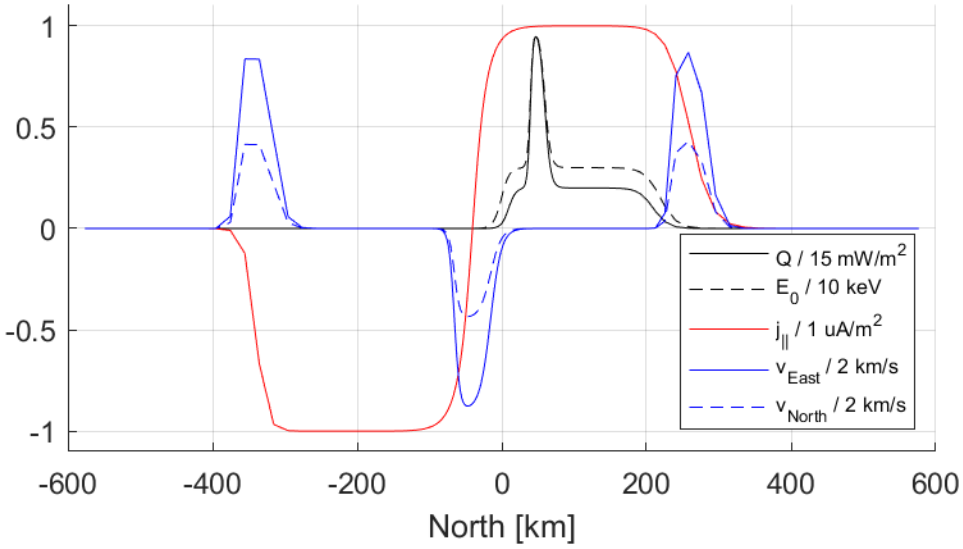

Figure 2: A central north-south cut of parameters for a set of GEMINI input maps. Values are normalized to their respective maxima. Some resolution artifacts are seen near the edges of the model space as this spatial grid has a coarser cell spacing at the boundaries.

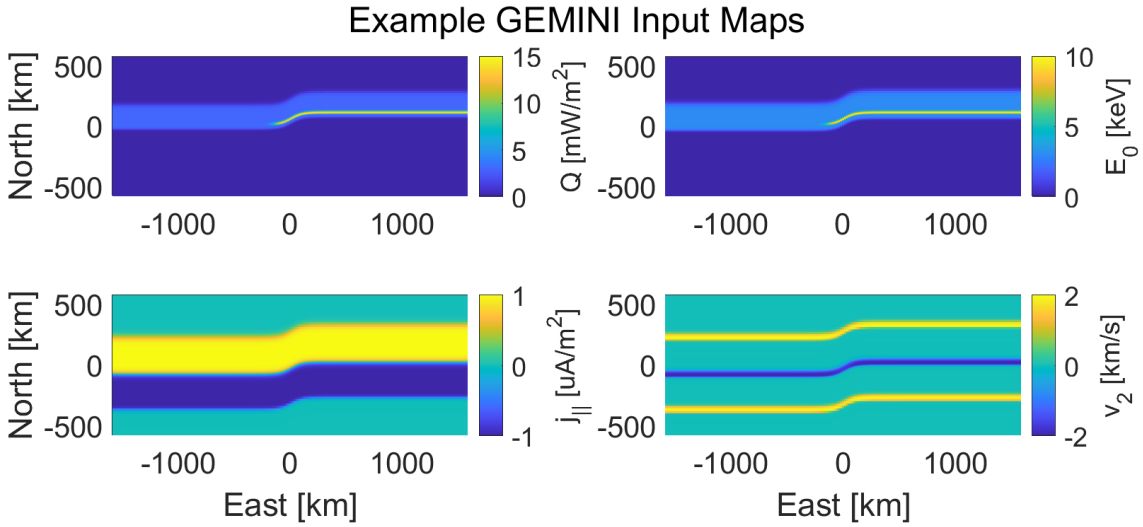

Figure 3: 2-D input maps from Figure 2. Only the eastward component of the $\mathbf{E} \times \mathbf{B}$ flow is shown, yet ultimately the potential map relating to this electric field is used.

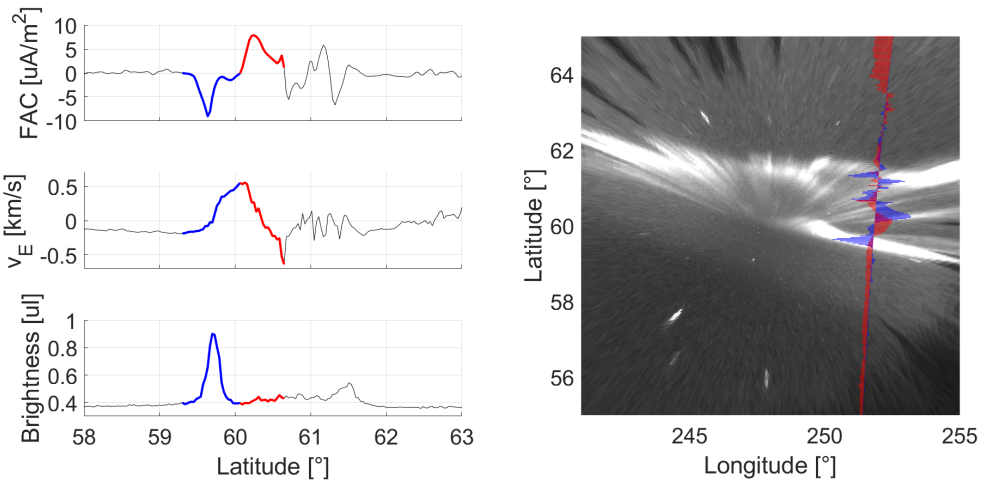

Figure 4: A stereotypical example of an up-down current pair crossing by Swarm C from April 22, 2014 along with cross-track flow data and the associated brightness provided by the Fort Smith THEMIS all-sky imager. This particular crossing is post-midnight at around 1 MLT. Blue/red shading represent the precipitation/return currents. The image spacecraft data overlay has FAC in blue and cross-track flow in red. On the image, vectors pointing right indicated eastward cross-track flow and downward (return) FAC. The compilation of this figure was made using data reduced by A. Mule and M. S. Kawamura (Data available at `http://themis.ssl.berkeley.edu/gmag/`, `https://aurorax.space/`, `https://earth.esa.int/eogateway/missions/swarm/data`).

were a flow driven one, an example of associated flow is shown as well. In addition to all this, a more intense sheet of precipitation is added which traces the profile westward at 3 km/s. This example illustrates the level of along-arc spatiotemporal structure that will be introduced as a means to stray from idealized, sheet-like arcs. The idea of replicating across-arc cuts of data along an arc contour comes from work done by Clayton et al. (2021).

The plasma flow driving map is converted to a potential map by "integrating" $\mathbf{v}_\perp = -\nabla\phi \times \mathbf{B}_0$. Previous code, originally used to reconstruct 2-D flow fields from multi-point spacecraft data has q been re-written to perform this task.

A note should be made that the precipitation spectrum from the calculations by (Fang et al., 2010) might not match the inverted-V description needed for this work. GEMINI is set up to use the GLobal airglOW (GLOW) model (Solomon, 2017), which will be used to compare against stereotypical electron energy spectrum data (FAST, etc.). A calculation choice will be made using this comparison.

The north-south cut shown in Figure 2 is a basic, speculative version of an arc system grounded in the thesis work done by Wu (2020). Part of this thesis will be to improve this picture based on

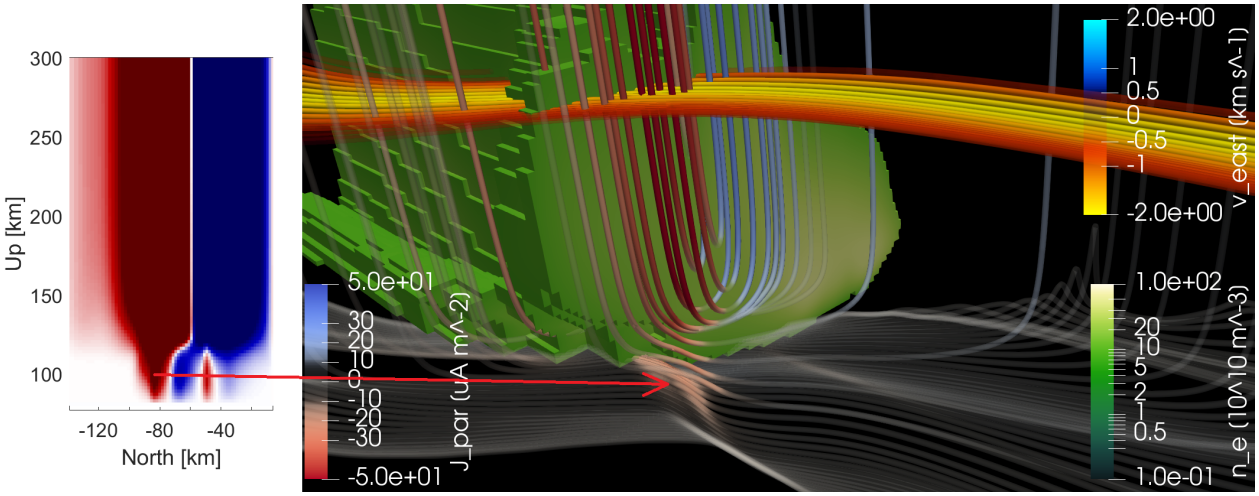

Figure 5: An example of a GEMINI output datacube rendered by ParaView and why 3-D visualization tools are needed. This run shows strong FAC produced by plasma flow shear penetrating enhanced density closing largely through Pedersen currents. However, some FAC is closed through Hall current at lower altitudes, with embedded FAC in the closure route caused by along-arc gradients of Hall conductance.

in-situ and ground-based data provided by A. Mule and M. S. Kawamura as part of their research in the *Lynch "317" Rocket Lab*. Figure 4 shows a stereotypical example from ESA's SWARM mission in conjunction with the THEMIS-GBO mission. A possible superposed epoch analysis of such examples is in the works, and will be a great asset to this work.

With the tools outlined above, a catalogue will be constructed of parameterized inputs of stereotypical flow, FAC, and precipitation cuts, each with minor along-arc structure. These inputs and their parameters will be systematically adjusted and built upon in order to compare the GEMINI outputs and investigate their effects. A script is set in place, developed by E. W. McManus, that is fed a list of parameters that determine the morphology of an input function which then provides the input folder structure needed to run GEMINI. This script also allows for a particular input folder structure to be copied with sequential changes to particular parameters.

3.3 Visualization

Properly interpreting 3-D data requires 3-D visualization, especially in terms of determining the path of current continuity. Figure 5 shows GEMINI output data rendered using ParaView (Ayachit, 2015) along with a 2-D latitudinal cut of that same FAC data. The FAC dip reaching down into the E-region clearly is shown to have a very different closure path than that of the main Pedersen

closure as marked by the red arrow. Interestingly, this visualization does not match up with the 2-D current loop description made by Mallinckrodt (1985) from this perspective. To facilitate the GEMINI output comparison, standardized 3-D visualization views are under development using these techniques.

3.4 Modular GEMINI Additions

3.4.1 Quasi-Static Induction Module

Currently the GEMINI model can handle timescales of ∼100 s in order to keep accurate assumptions. To bring this down to ∼10 s the model would require certain inductive effects (Lotko, 2004; Richmond, 2010). Inductive MI coupling is not negligible in DC auroral system science, and in order to better understand when these effects can be ignored in auroral arc current continuity, a module will be developed as an addition to the GEMINI model that includes induction while retaining the quasi-static assumptions (Lotko, 2004). A possible path to do this would require the following fundamental changes to the scripts handling Maxwell's and fluid equations (Zettergren, personal communication, April 22, 2022):

1. The perpendicular ion momentum density will require the full time-dependent treatment.
2. The full electron momentum density will also require the full time-dependent treatment.
3. Instead of current continuity, $\nabla \cdot \mathbf{j} = 0$, the current density will be calculated via $\mathbf{j} = \sum_s n_s q_s \mathbf{v}_s$ with s being the electrons and all 6 ion species.
4. With this a time-dependent magnetic field through $\nabla \times \mathbf{B} = \mu_0 \mathbf{j}$ is determined.
5. The electric field will be calculated through $\nabla \times \mathbf{E} = \partial_t \mathbf{B}$ instead of through Ohm's law, as it is now.

Whether these changes will provide a closed system of equations is still an active discussion at the time of writing this document. Furthermore, the new active scale sizes involved will most likely require a much denser grid. To stay within the context of mesoscale auroral system science, this will likely require 2-D simulations at first.

3.4.2 Poynting Theorem Constraint Module

A possible second module to be added to the GEMINI model will include some form of bookkeeping the electromagnetic energy and its dissipation through Joule heating. Not only will this help in investigating the energy flow of the 3-D Cowling channel presented by Fujii et al. (2011), but this would also allow for a Poynting's theorem constraint which will ultimately help determine the physical solution to the current continuity equation. This, however, is not as easy as it sounds and will require extensive research in how the ionosphere deals with Poynting flux, starting with an in-depth read of a study by Richmond (2010).

4 Science Studies

With the tools and methods described in the previous section, a number of science studies will be carried out. As a baseline simulation, a basic cut, such as the one shown in Figure 2, will replicate along a straight contour with no along-arc variation where one run will be FAC driven and one will be flow driven. This will not only provide a proper output for comparison, but also tell us what GEMINI simulates as the flow cut for a FAC driven run and vice versa. Such cuts can be used to drive GEMINI in additional runs. From this, various different across-arc cuts and along-arc contour definitions will be catalogued. A preliminary list of such simulations includes:

- A straight-contour run with more intense precipitation that reaches down to lower altitudes where Hall conductivity peaks. This will show how much more likely and what portion of FAC will close through Hall current with no along-arc gradients.
- A basic run but with a bent-contour. This will show if minor along-arc structure will change the path of current closure.
- A bent contour that surges westward. Studying the current closure in the wake of the bent profile will show the ways in which straggling recombination along with transport will introduce various artifacts.
- More intense precipitation embedding itself onto the less intense precipitation gradually over time. This will provide insight into how introducing intense auroral precipitation affects current closure inside the Cowling channel as it transitions.

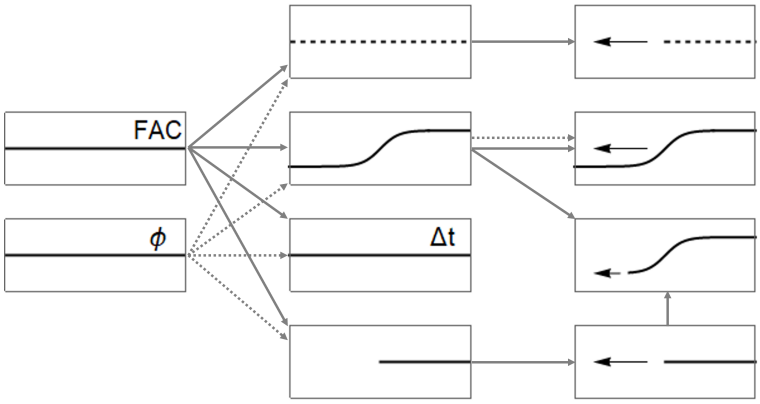

Figure 6: A catalogue of various driver map contours. The dashed contours indicate lower reaching precipitation, the "Δt" indicates slowly increasing precipitation, and the black arrows indicate contour motion. Dashed arrows indicate potential driven runs.

- A short arc (sharc). This has the intense precipitation diminish along the arc direction over some gradient scale length. This will provide a means of determining how the low to high intensity precipitation transitions in space.

Along with these runs there will be various other combinations of these morphologies. Figure 6 shows an early rendition flow chart of such simulations. Each case in this figure will itself include several runs where the parameters relevant to that input are gradually adjusted. E.g. the precipitation characteristic energy or the slope of the bend can be changed in finite steps from their baselines.

Another study will be done after an implementation of GEMINI induction has been properly tested. A comparative study will look into the dependence of current closure to Alfvénic coupling. A possible first candidate would include a 2-D baseline input simulation with the original GEMINI configuration, one with the new inductive GEMINI configuration but with the induction suppressed, and then one with the full inductive treatment. This treatment can then be performed on more complex runs which ultimately will determine a metric for when inductive effects are non-negligible.

A current path to science closure will include the development of metrics for these science studies to make concrete conclusions on the dependence of the input and output parameters. E.g. a metric to determine the fraction of FAC closed in a particular region by Pedersen versus Hall current plotted against the degree of bend in an arc contour. This enables one to make conclusions on the energy dissipation of an arc based on imagery alone.

5 Tasks and Goals

5.1 Finished Work

This dissertation grows out of my work on the Auroral Reconstruction CubeSwarm (ARCS) concept study report. This partly involved the study of numerous Observing System Simulation Experiments (OSSEs) which had mock spacecraft gather data through a GEMINI simulated model space and seeing how well they could reconstruct it from their in-situ data. One of my tasks, which built on substantial preliminary work done by T. Evans and A. Mule et al., was to reconstruct the 2-D perpendicular flow space. In doing this, I became familiar with GEMINI as well as visualization tools like ParaView. Incidentally, the flow reconstruction script I wrote provides a tool for converting flow maps into potential maps, after having made a few adjustments. This script will be used in this work.

At the AGU Fall Meeting of 2021 I presented work on "The Effect of Hall Conductance Gradients in Non-Sheet-Like Auroral Arcs on Field-Aligned Currents" (van Irsel et al., 2021a). This study involved an OSSE much like the second-from-the-top, right-most case in Figure 6. In this work I conclude that "westward moving auroral arc systems with minor bends can cause conductivity signatures which source along-arc, up-down pairs of ionospheric FAC contributed from along-arc gradients in Hall conductance".

At the 2021 CEDAR Workshop I presented "FAC Contributions from Hall Conductance Gradients in Non-Sheet-Like Auroral Arcs" (van Irsel et al., 2021b). This work was preliminary to the work above and focused on straggling recombination of the electron density plume in the wake of the bend.

In the winter of 2021 I helped build, tested, and successfully integrated plasma instrumentation (Petite Ion Probes (PIPs)) onto the Loss through Auroral Microburst Pulsation (LAMP) sounding rocket mission. This work included space plasma environment testing, on-site integration at the Poker Flat Research Range in Alaska, and provided me with a more intimate understanding of both space weather predictions, as well as the aurora themselves, during the nights of the launch window. The idea for the *sharc* run was sown during one of these nights as we saw short, discrete arcs surge westward across the sky.

5.2 Unfinished Work

The following is an itemized list of tasks that I will focus on throughout my remaining academic years working toward my doctorate. Naturally, these will be subject to change.

5.2.1 Academic Year 3

- I will conclude this thesis proposal work and present it to my committee.
- A discussion will be had regarding the path to a closed system of equations allowing induction in GEMINI with M. D. Zettergen.
- A version of the *sharc* simulation will be run and I will present any findings at the 2022 CEDAR Workshop in June.

5.2.2 Academic Year 4

- Appropriate inverted-V precipitation calculations to provide GEMINI will be settled on, whether using those by Fang et al. (2010) and/or those provided by GLOW, or through some other means.
- I will investigate the superposed epoch analysis by A. Mule and M. S. Kawamura and a list of stereotypical across-arc cuts of FAC, flow, and precipitation will be tentatively settled on.
- I will publish a short paper on the reconstruction algorithm used in the ARCS concept study report.
- A catalog of GEMINI runs will be studied and I will publish a paper on any findings made.
- With the help of M. D. Zettergren, I will implement the induction model into GEMINI and do a comparative study.
- I will develop and submit proposals for graduate funding to the NSF and/or the GSRP.
- I will attend and present at the 2022 AGU Fall meeting and the 2023 CEDAR Workshop.
- I will aim to pass PHYS 76: *Methods of Experimental Physics* in order to fulfil my candidacy requirements.

5.2.3 Academic Year 5

- I will publish a paper on the comparative GEMINI induction study.

- I will attend and present at the 2023 AGU Fall meeting and the 2024 CEDAR Workshop.

- I will finish writing my dissertation and defend it if all goes to plan.

5.3 Postface

The writing of this proposal has provided me with much clarity and excitement toward the future of this project. The numerous projects I've worked on in the past 3 years have given me plenty of valuable knowledge and experience. This document has given me an opportunity to sift through this work and has cleared up a pathway to what I believe will be compelling science. I would like to take this time to thank Kristina Lynch for her invaluable advice and mentoring, as well as the help and support from the entire 317 Lab team without whom this work would not be possible.

References

Amm, O., Aruliah, A., Buchert, S. C., Fujii, R., Gjerloev, J. W., Ieda, A., Matsuo, T., Stolle, C., Vanhamäki, H., and Yoshikawa, A. (2008). Towards understanding the electrodynamics of the 3-dimensional high-latitude ionosphere: present and future. *Annales Geophysicae*, 26(12):3913–3932.

Archer, W. E., Knudsen, D. J., Burchill, J. K., Jackel, B., Donovan, E., Connors, M., and Juusola, L. (2017). Birkeland current boundary flows. *Journal of Geophysical Research: Space Physics*, 122(4):4617–4627.

Ayachit, U. (2015). *The ParaView Guide: A Parallel Visualization Application*. Kitware, Inc., Clifton Park, NY.

Brekke, A. (1989). Auroral ionospheric conductances during disturbed conditions. *Annales Geophysicae*, 7:269–280.

Clayton, R., Burleigh, M., Lynch, K. A., Zettergren, M., Evans, T., Grubbs, G., Hampton, D. L., Hysell, D., Kaeppler, S., Lessard, M., Michell, R., Reimer, A., Roberts, T. M., Samara, M., and Varney, R. (2021). Examining the auroral ionosphere in three dimensions using reconstructed 2D maps of auroral data to drive the 3D GEMINI model. *Journal of Geophysical Research: Space Physics*, 126(11).

Cowley, S. W. H. (2000). Magnetosphere-ionosphere interactions: A tutorial review. *Magnetospheric Current Systems, Geophysical Monograph Series*, 118:91–106.

Dungey, J. W. (1961). Interplanetary magnetic field and the auroral zones. *Physical Review Letters*, 6:47–48.

Ergun, R. E., Carlson, C. W., McFadden, J. P., Mozer, F. S., Muschietti, L., Roth, I., and Strangeway, R. J. (1998). Debye-scale plasma structures associated with magnetic-field-aligned electric fields. *Physical Review Letters*, 81:826–829.

Evans, D. S. (1974). Precipitating electron fluxes formed by a magnetic field aligned potential difference. *Journal of Geophysical Research*, 79(19):2853–2858.

Fang, X., Randall, C. E., Lummerzheim, D., Wang, W., Lu, G., Solomon, S. C., and Frahm, R. A. (2010). Parameterization of monoenergetic electron impact ionization. *Geophysical Research Letters*, 37(22).

Fraunberger, M., Lynch, K. A., Clayton, R., Roberts, T. M., Hysell, D., Lessard, M., Reimer, A., and Varney, R. (2020). Auroral ionospheric plasma flow extraction using subsonic retarding potential analyzers. *Review of Scientific Instruments*, 91(9).

Fujii, R., Amm, O., Yoshikawa, A., Ieda, A., and Vanhamäki, H. (2011). Reformulation and energy flow of the Cowling channel. *Journal of Geophysical Research: Space Physics*, 116(A2).

Goertz, C. K. and Boswell, R. W. (1979). Magnetosphere-ionosphere coupling. *Journal of Geophysical Research: Space Physics*, 84(A12):7239–7246.

Grubbs, G., Michell, R., Samara, M., Hampton, D., Hecht, J., Solomon, S., and Jahn, J. (2018). A comparative study of spectral auroral intensity predictions from multiple electron transport models. *Journal of Geophysical Research: Space Physics*, 123(1):993–1005.

Kaeppler, S. R., Kletzing, C. A., Rowland, D. E., Jones, S., Heinselman, C. J., Bounds, S. R., Gjerloev, J. W., Anderson, B. J., Korth, H., LaBelle, J. W., Dombrowski, M. P., Lessard, M., and Pfaff, R. F. (2012). Current closure in the auroral ionosphere: Results from the auroral current and electrodynamics structure rocket mission.

Karlsson, T., Andersson, L., Gillies, D., Lynch, K., Marghitu, O., Partamies, N., Sivadas, N., and Wu, J. (2020). Quiet, discrete auroral arcs-observations. *Space Science Reviews*, 216(1):1–50.

Kelley, M. C. (2009). *The Earth's ionosphere: plasma physics and electrodynamics*. International Geophysics Series, v. 96. Academic Press, Amsterdam, Netherlands, 2nd edition.

Knight, S. (1973). Parallel electric fields. *Planetary and Space Science*, 21(5):741–750.

Lotko, W. (2004). Inductive magnetosphere-ionosphere coupling. *Journal of Atmospheric and Solar-Terrestrial Physics*, 66(15):1443–1456.

Lühr, H., Park, J., Gjerloev, J. W., Rauberg, J., Michaelis, I., Merayo, J. M. G., and Brauer, P.

(2015). Field-aligned currents' scale analysis performed with the Swarm constellation. *Geophysical Research Letters*, 42(1):1–8.

Lysak, R. L. (1985). Auroral electrodynamics with current and voltage generators. *Journal of Geophysical Research: Space Physics*, 90(A5):4178–4190.

Mallinckrodt, A. J. (1985). A numerical simulation of auroral ionospheric electrodynamics. *Journal of Geophysical Research: Space Physics*, 90(A1):409–417.

Marghitu, O. (2012). Auroral arc electrodynamics: Review and outlook. *Relationship between auroral phenomenology and magnetospheric processes: Earth and oher planets, Geophysical Monograph Series*, 197:143–158.

Paschmann, G., Haaland, S., and Treumann, R. (2003). *Auroral Plasma Physics*. Springer Netherlands, Dordrecht, Netherlands.

Richmond, A. D. (2010). On the ionospheric application of Poynting's theorem. *Journal of Geophysical Research: Space Physics*, 115(A10).

Rother, M., Schlegel, K., and Lühr, H. (2007). CHAMP observation of intense kilometer-scale field-aligned currents, evidence for an ionospheric Alfvén resonator. *Annales Geophysicae*, 25(7):1603–1615.

Seyler, C. E. (1990). A mathematical model of the structure and evolution of small-scale discrete auroral arcs. *Journal of Geophysical Research: Space Physics*, 95(A10):17199–17215.

Solomon, S. C. (2017). Global modeling of thermospheric airglow in the far ultraviolet. *Journal of Geophysical Research: Space Physics*, 122(7):7834–7848.

Sugiura, M., Maynard, N. C., Farthing, W. H., Heppner, J. P., Ledley, B. G., and Cahill Jr., L. J. (1982). Initial results on the correlation between the magnetic and electric fields observed from the DE-2 satellite in the field-aligned current regions. *Geophysical Research Letters*, 9(9):985–988.

Temerin, M. and Carlson, C. W. (1998). Current-voltage relationship in the downward auroral current region. *Geophysical Research Letters*, 25(13):2365–2368.

van Irsel, J., McManus, E., Burleigh, M., Lynch, K. A., and Zettergren, M. D. (2021a). The effect of Hall conductance gradients on field-aligned currents in non-sheet-like auroral arcs. In *2021 AGU Fall Meeting*, New Orleans, LA. American Geophysical Union.

van Irsel, J., McManus, E., Burleigh, M., Lynch, K. A., and Zettergren, M. D. (2021b). FAC contributions from Hall conductance gradients in non-sheet-like auroral arcs. In *2021 CEDAR Workshop*, Virtual. CEDAR.

Wolf, R. A. (1975). Ionosphere-magnetosphere coupling. *Space Science Reviews*, 17(2):537–562.

Wu, J. (2020). *Static and Alfvénic Electrodynamics in the Auroral Region*. PhD thesis, University of Calgary, Calgary, Canada.

Wygant, J. R., Keiling, A., Cattell, C. A., Johnson, M., Lysak, R. L., Temerin, M., Mozer, F. S., Kletzing, C. A., Scudder, J. D., Peterson, W., Russell, C. T., Parks, G., Brittnacher, M., Germany, G., and Spann, J. (2000). Polar spacecraft based comparisons of intense electric fields and poynting flux near and within the plasma sheet-tail lobe boundary to UVI images: An energy source for the aurora. *Journal of Geophysical Research: Space Physics*, 105(A8):18675–18692.

Zettergren, M. D. (2022). personal communication.

Zettergren, M. D. and Semeter, J. L. (2012). Ionospheric plasma transport and loss in auroral downward current regions. *Journal of Geophysical Research: Space Physics*, 117(A6).

Zettergren, M. D., Semeter, J. L., and Dahlgren, H. (2015). Dynamics of density cavities generated by frictional heating: Formation, distortion, and instability. *Geophysical Research Letters*, 42(23):10120–10125.